



# DEVELOPMENT AND CHARACTERIZATION OF RIFABUTIN LOADED TARGETED POLYMERIC NANOPARTICLES FOR EFFECTIVE DELIVERY IN LUNGS

Anamika Mary David<sup>1</sup>, Dr. Rupal Dubey<sup>1\*</sup>, Dr. Bhaskar Gupta<sup>1</sup>, Khushboo Mehandole<sup>1</sup>

<sup>1</sup>School of Pharmacy and Research, Peoples University, Bhopal, MP

**ABSTRACT-** The present research study was objected towards development and evaluation the mannosylated Rifabutin loaded polymeric nanoparticles for effective delivery in lungs. Preformulation studies are carried out to ensure the development of a stable as well as therapeutically effective and safe dosage form. FTIR analysis was performed in order to confirm the drug and excipient interaction. In spectra of a mixture there are no peaks other than the typical peak found which show they are compatible. RIF exhibits excellent solubility in chloroform with a solubility of 55.87 gm per litre. The particle size decreases steadily along with higher amount of glutaraldehyde applied was approximately reduction in particle size from  $421 \pm 6.02$  nm to  $204 \pm 3.4$  nm for RIF. In contrast PDI ( $0.19 \pm 0.017$ ) was found minimum at GNP4 glutaraldehyde. The 2 percent concentration of gelatin with average size  $267 \pm 12.72$  (nm) and entrapment efficiency of  $58.2 \pm 4.1$  with PDI  $0.22 \pm 0.015$  was selected to prepare mannosylated gelatin nanoparticles. The MN-GNPs was formulated having size  $417 \pm 31.4$  with drug entrapment efficiency of  $52.4 \pm 1.68$  hence responsible for lower drug entrapment as compared to plain nanoparticles. SEM was employed and surface of the both types of gelatin nanoparticles was found to be smooth. TEM study showed that GNPs and MN- GNPs were found to be spherical in shape and size within nanometric range. The in- vitro drug release profile were studied using dialysis membrane. The GNP formulation showed  $94 \pm 6.38\%$  drug release in 120 hrs whereas the MN-GNPs showed  $84.64 \pm 5.76\%$  RIF release at the end of 120 hrs. The Ex- vivo studies showed cellular uptake of FITC loaded GNPs that with RIF loaded MN-GNPs high drug concentration can be achieved in alveolar macrophages. The MTT cytotoxicity of RIF loaded MN-GNPs was 0.326 found  $10.81 \pm 0.9\%$  hemolysis after 1 hour. The result of research after preformulation studies of MN GNPs may therefore be feasible and successful option for the regulated and safe administration of RIF in targeted drug delivery to lungs for treatment of Tuberculosis.

**Key Words:** Rifabutin, Targeted polymeric nanoparticles, Tuberculosis,

## INTRODUCTION

Mycobacterium tuberculosis, which causes TB, is a chronic infectious illness that has infected over a billion people globally.

In the nation's most severely impacted by AIDS, the incidence of TB has increased significantly as a result of HIV-1 infection. The first-line antitubercular medicines (ATDs) Rifampicin (RIF), Isoniazid (INH), and Pyrazinamide (PYZ) were employed for current frontline treatment of tuberculosis. For oral administration in the initial phase, three doses of INH, RIF, and PYZ per week for two months was indicated by the specifically observed short course of treatment (DOTS). These first-line antitubercular medications have a number of drawbacks, including drug resistance, liver damage, gastrointestinal problems, rashes, etc. The growth of multidrug resistant TB has highlighted both the necessity for the development of novel TB drug therapies and the shortcomings of the current conventional TB treatment, especially the lengthy duration of the treatments and the issues with patient compliance. This made formulation scientists more motivated to create nanoparticulate delivery systems for better disease control.

Nanoparticles (NPs) are solid dispersions or particles with a size between 10 and 1000 nm. The medication is broken down, trapped, encapsulated, or bound using a nanoparticle matrix.

Nanoparticles can be a helpful strategy for treating tuberculosis (TB) in two different ways: (i) for their inherent antimycobacterial activity; and (ii) as vehicles for well-known antitubercular drugs to reduce dosage and drug-associated side effects and allow administration via convenient administration routes like pulmonary or oral ones. A wide range of nanocarriers, including polymeric nanoparticles, nanocapsules, micelles, dendrimers, nanogels, and liposomes, have been designed to access the reservoirs of Mtb. By physical encapsulation, adsorption, or chemical conjugation, therapeutic agents can be added to nanocarriers. The ability of gelatin nanoparticles to lessen the toxicity associated with the majority of medications makes them one of the most promising options for regulated pharmaceutical release. The biocompatible polymers that make up gelatin are produced from the collagen that is present in animal skin and bones. (19) Therefore, the goal of the current work was to create gelatin nanoparticles containing rifabutin for the treatment of TB.

## MATERIALS AND METHODS

### Material-

#### Materials and their sources

S. No.	Ingredients	Sources
1.	Rifabutin	Lupin Ltd., Pune
2.	Gelatin	S D Fine Chem Ltd., Indore
3.	Dichloromethane	Rankem (Sugandha Enterprises Paonta Shahib H.P.)
4.	Methanol	Rankem (Sugandha Enterprises Paonta Shahib H.P.)
5.	Chloroform	Rankem (Sugandha Enterprises Paonta Shahib H.P.)
6.	n-octanol	Sugandha Enterprises Paonta Shahib H.P.
7.	HPLC grade water	Sigma-Aldrich, Mumbai
8.	HPLC grade acetonitrile	Rankem (Sugandha Enterprises Paonta Shahib H.P.)
9.	Pot di hydrogen phosphate	S D Fine Chem Ltd., Indore
10.	Di-sod hydrogen phosphate	S D Fine Chem Ltd., Indore

Instruments required for the preparation of GNPs

S. No.	Instrument	Company/ Model
1.	Digital electronic balance	Shimadzu, Japan
2.	pH measurements	Scope enterprise New Delhi
3.	FTIR spectrophotometer	Shimadzu FTIR modal IR Afinity-IS (Japan)
4.	UV- Visible spectrophotometer	Systronics double beam spectrophotometer 2203
5.	Dissolution test apparatus	Electrolab Ltd., Mumbai, India
6.	Stability control oven	Thermolab, Mumbai, India
7.	Melting point apparatus	Labtronics, Haryana
8.	Sonicator	Labtronics, Haryana

## DRUG PROFILE (RIFABUTIN)

Generic Name: Rifabutin

Chemical names:

a) 1',4-didehydro-1-deoxy-1,4-dihydro-5'-(2-methylpropyl)-1- oxorifamycin XIV

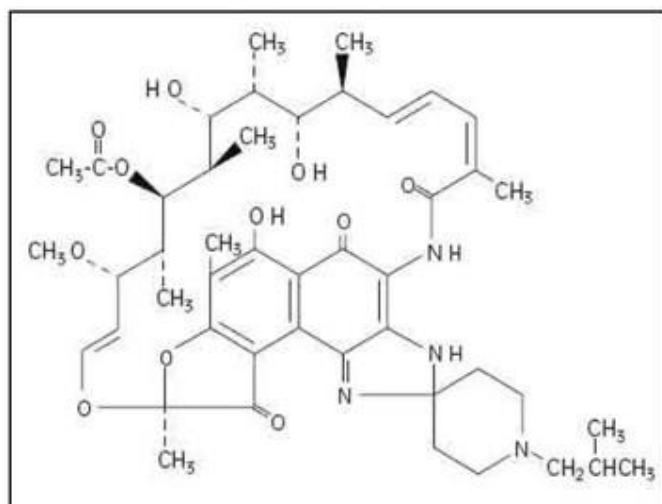
b) (9S, 12E, 14S, 15R, 16S, 17R, 18R, 19R, 20S, 21S, 22E,

24Z)-6,16,18,20-tetrahydroxy-1'isobutyl-14-methoxy-7,9,15,17,19,21,25-heptamethyl-spiro[9,4 (epoxy)pentadeca[1,11,13]trienimino)-2H-furo[2',3':7,8]naphth[1,2-d]imidazole-2,4'-piperidine]-5,10,26-(3H,9H)-trione-16-acetate.

**Molecular Weight:** 847.02

**Molecular formula:** C<sub>46</sub>H<sub>62</sub>N<sub>4</sub>O<sub>11</sub>

**Structural Formula:**



Chemical structure of Rifabutin

**Description:** Red-violet powder

### Antibacterial activity

About one-third of the rifampicin-resistant *M. tuberculosis* strains may be treated with rifabutin. The minimum inhibitory concentration (MIC) for *Mycobacterium TB* was found to be 0.006 mg/l for rifampicin-sensitive strains and 6-16 mg/l for rifampicin-resistant strains. The MICs for resistant strains are much higher than clinically achievable concentration in blood (C max-0.5 mgA blood after 300 mg given orally; C max 3 mg/l in lung tissues

### Dose (Pharmacia, USP)

The usual oral adult dose of rifabutin is 300 mg once a day.

Side effects:

- Severe skin rash or itching.
- Pale skin, weakness, easy bruising/ bleeding.
- Fever, chills, body aches, flu symptoms or eye pain or redness, vision loss.
- Red, orange, brown discoloration of your skin, tears, sweat, saliva, urine, or stools.
- Headache, Nausea, vomiting, diarrhea.
- Stomach pain.
- Belching, bloating, loss of appetite.
- Mild skin rash or itching.

### Therapeutic Uses:

Rifabutin is used for the treatment of pulmonary tuberculosis.

- Useful against some isolates of MDR TB.
- Disseminated atypical mycobacterium infection in AIDS patients with multidrug-resistant tuberculosis may be prevented and treated effectively. In HIV patient, the substitution of rifabutin for rifampicin minimizes drug interaction with the HIV protease inhibitors and non- nucleoside reverse transcriptase inhibitors.

### POLYMER PROFILE (GELATIN)

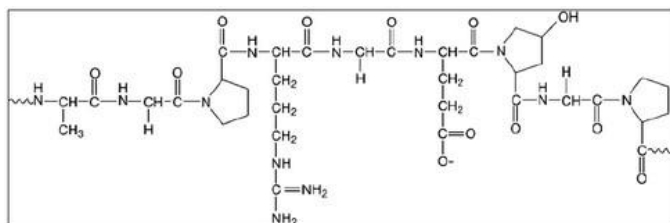
**Synonyms:** Byco; Crysogel; E441; gelatin; instagel; kolatin; solugel; vitagel

**Chemical names:** Gelatine [9000-70-8]

**Molecular Weight:** Varying from 2000 – 200000.

**Molecular formula:** The protein fractions consist almost entirely of amino acids joined together by amide linkages form linear polymers.

**Description:** Light-amber to faintly yellow-colored, brittle solid.



Structure of gelatin

## Characterization of nanoparticles

The prepared gelatin nanoparticles were characterized for Particle size, Surface charge, Particle Morphology, Surface Morphology, % Drug entrapment and In-vitro Drug Release study. Using a Zetasizer (DTS Ver. 4.10, Malvern Instruments, England), photon correlation spectroscopy was utilized to determine the average particle size and polydispersity index of the GNPs. Using laser Doppler anemometry and a Malvern Zetasizer (also known as a Doppler Electrophoretic Light Scatter Analyzer), the zeta potential of the nanoparticles was assessed. To see the particle morphology, a transmission electron microscope (TEM) was employed. At MANIT, Bhopal, a scanning electron microscope (SEM) was used to analyse the surface morphology. A Sephadex micro column was used to determine the amount of drug entrapment. Using a dialysis tube, it was possible to measure the in vitro drug release of the GNPs formulation's trapped rifabutin.

## METHODS-

**Preformulation studies-** To assure the creation of a stable dosage form that is also therapeutically efficacious and safe, preformulation studies are required. Rifabutin was used in this investigation to identify the drug. A little amount of the drug powder was placed on butter paper and examined in an area with adequate illumination. Rifabutin's melting point was then determined using a melting point equipment (Tempo, Mumbai). FTIR Spectroscopy was used to establish the drug's excipient compatibility study. Lansoprazole estimation was carried out using UV-Visible Spectrophotometry. For the quantitative assessment of the medication, a spectrophotometric calibration curve was created based on UV absorption at a maximum wavelength of 275 nm in PBS pH 6.8. The sample was qualitatively tested for its solubility in various solvents and the partition behavior of drug was examined in n-octanol: water, n-octanol: PBS (7.4) system.

## Formulation of gelatin nanoparticles (GNPs) –

In order to create nanoparticles, double desolvation was used. In 10 ml of water, 0.2 gm (2.0%) of gelatin was dissolved by keeping the temperature at 40°C. The high molecular mass (HMM) gelatin was then precipitated by adding 10 ml of acetone as a desolvating agent to 10 ml of gelatin solution. After discarding the supernatant, the HMM was once again dissolved in 10 ml of distilled water while being constantly stirred at 1200 rpm. With the aid of HCl, the pH of the solution was then adjusted to 3.0. The medicine solution, which was 0.1% w/w, was then added. By adding acetone drop by drop and stirring for 30 minutes at 1200 rpm with a magnetic stirrer, the gelatin was re-desorbed. The developed gelatin nanoparticles were cross-linked with 200µl of room-temperature aqueous glutaraldehyde solution (25%, v/v), while being agitated at 1200 rpm for 12 hours. We first used cysteine to neutralise the excess before sonicating the glutaraldehyde-free nanoparticles for 2.0 minutes. The particles were cleaned after centrifugation at 10,000 rpm for 20 minutes, and the cleaned nanoparticles were kept cool. (23)

**Optimization of formulations:** Gelatin and glutaraldehyde concentration were optimised. In order to achieve nanometric size, low polydispersity index (PDI), and maximum drug entrapment effectiveness, the effects of these factors were observed. (24) Table-1 lists various formulation variables along with their formulation codes

**Optimization of formulations: Gelatin and gluteraldehyde concentration were optimised.**

S. No.	Formulation code	Variables	Values
1.	GNP 1	Volume of crosslinking agent (Gluteraldehyde)	50 µl
	GNP 2		100 µl
	GNP 3		200 µl
	GNP 4		300 µl
	GNP 5		400 µl
	GNP 6		500 µl
2.	GNP 7	Gelatin Concentration	1%
	GNP 8		2%
	GNP 9		4%
	GNP 10		8%

**STABILITY STUDIES-**

To find out whether drugs leached from gelatin during storage, a physical stability test was conducted. The samples were kept in glass vials and held for a month at two different temperatures, namely room temperature (25°C) and refrigerated temperature (4-8°C), with samples being taken at regular intervals. By evaluating the formulations' encapsulation effectiveness, the drug leakage from those formulations was examined.

*Ex-vivo studies*

Cellular uptake of fluorescein isothiocyanate (FITC) loaded GNPs: Macrophage cell lines J774 was used for cellular uptake study. The uptake study was performed at 1, 2 and 6 hours interval.

MTT cytotoxicity assay: 774 cells were resuspended in new growth media at a concentration of 1X10<sup>3</sup> cells/ml. By using a 3-(4,5-dimethylthiazol-2-yl)-5-diphenyl tetrazolium bromide (MTT) (Sigma Aldrich) colorimetric assay, the materials' capacity to suppress cell growth was assessed.

Hemolytic Toxicity: The study was carried out on whole human blood, which was collected in Hi-Anticlot vials (Himedia, India). The degree of hemolysis was determined by the following equation:

$$\text{Hemolysis (\%)} = \frac{\text{Abs} - \text{Abso}}{\text{Abs100} - \text{Abso}} \times 100$$

where Abs, Abs100, and Abso are the absorbances of sample, solution of 100% hemolysis, and solution of 0% hemolysis; respectively.

**RESULTS****Preformulation studies:**

Preformulation research aimed to create a database of knowledge on the pharmacological substance

Identification of Drug: Identification studies showed that the drug supplied by Lupin Pharma Pvt.Ltd, Pune

Parameters	Rifabutin (RIF)	Results
Appearance	Red-violet, crystalline, hygroscopic powder	Complies
Odor	Odorless	Complies

### Melting point of drug:

A capillary melting point method was used to determine the melting point of the drug. It was observed that the melting point of Rifabutin was found to be  $153 \pm 20$  C.

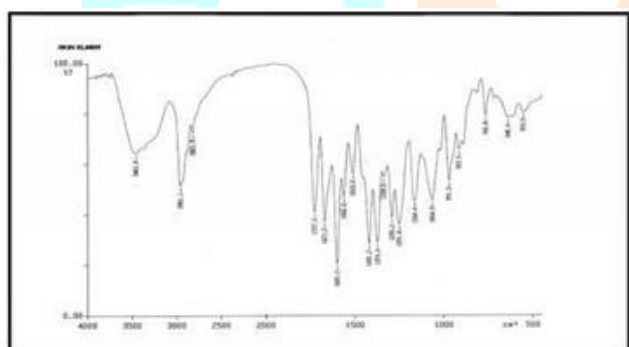
### FTIR spectroscopy of drug:

FTIR spectra of Rifabutin was obtained and compared with reference IR spectra for identification and confirmation of various functional groups.

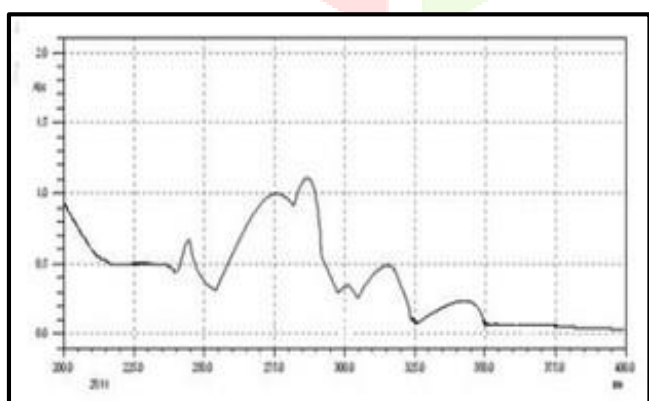
Important band frequencies in FTIR spectrum of Rifabutin

S.No.	IR Absorption band $\text{cm}^{-1}$	Assignments
1.	3461.0	O-H stretching (Alcohol, ROH)
2.	2961.1	Aliphatic C-H stretch
3.	2821.9	C-H stretch (Carboxylic acid)
4.	1727.3	C=O stretch of aldehyde
5.	1671.2	C=O stretch (cyclic amide)
6.	1601.2	C=C stretch Benzene (aromatic)
7.	1526.6	Asymmetric ( $\text{ArNO}_2$ ) stretch
8.	1421.2	O-H bending (Carboxylic acid)
11.	1064.9	C-N stretch (Amine)
12.	1164	C-O stretch (3 ROH)

Fig 1 FTIR spectrum of Rifabutin



Determination of wavelength maxima ( $\lambda_{\text{max}}$ ) and Calibration Curve of drug: UV spectra of drug were obtained by scanning drug solutions ( $10 \mu\text{g/ml}$ ) showed maximum absorption at 275 nm (Fig 2).

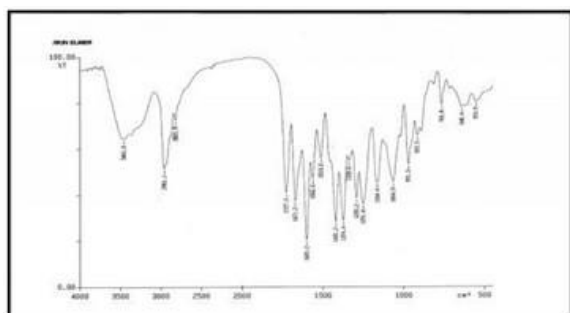


UV scan of Rifabutin drug sample

Calibration curve was prepared in PBS pH 7.4 at 275nm and linearly regressed. The correlation coefficient for standard curves was found to be very near to one which indicates good co-linear correlation between concentration  $2\text{-}20 \mu\text{g/ml}$  (Table 4 and Fig. 3). Hence, drugs are following Beer Lambert Law in the above range.

S.No.	IR Absorption band $\text{cm}^{-1}$	Assignmens
1.	3461.0	O-H stretching (Alcohol, ROH)
2.	2961.1	Aliphatic C-H stretch
3.	2821.9	C-H stretch (Carboxylic acid)
4.	1727.3	C=O stretch of aldehyde
5.	1671.2	C=O stretch (cyclic amide)
6.	1601.2	C=C stretch Benzene (aromatic)
7.	1526.6	Asymmetric (ArNO <sub>2</sub> ) stretch
8.	1421.2	O-H bending (Carboxylic acid)
11.	1064.9	C-N stretch (Amine)
12.	1164	C-O stretch (3 ROH)

## 1 FTIR spectrum of Rifabutin



Determination of wavelength maxima ( $\lambda_{\text{max}}$ ) and Calibration Curve of drug: UV spectra of drug were obtained by scanning drug solutions (10  $\mu\text{g/ml}$ ) showed maximum absorption at 275 nm.

## Calibration curve of Rifabutin in PBS pH 7.4

Drug concentration (mg/ml)	Absorbance (Observed)	Absorbance (Regressed)	Statistical parameter
2	0.0513	0.0507	Equation of line: $y = 0.0252x + 0.0003$ $R^2 = 0.9991$
4	0.1064	0.1011	
6	0.1509	0.1515	
8	0.1987	0.2019	
10	0.2533	0.2523	
12	0.2979	0.3027	
14	0.3567	0.3531	
16	0.3991	0.4035	
18	0.4506	0.4539	
20	0.5129	0.5043	

## Solubility studies

It was determined in solvent (i.e., water, PBS pH 7.4, methanol, ethanol, ether, chloroform etc.).

S. No.	Solvent	Solubility (mg/ml)	Solubility
1	Water	0.0092	Insoluble
2	PBS (pH 7.4)	0.42	Slightly soluble
3	Methanol	0.49	Slightly soluble
4	Ethanol	0.96	Sparingly soluble
5	Ether	0.0075	Insoluble
6	Chloroform	55.87	Freely soluble

## Partition coefficient:

The partition coefficient of Rifabutin was determined in n- octanol: PBS pH (7.4) system. The partition coefficient of Rifabutin was found to be 2.7

Drug	Amount of Drug (mg)		Partition coefficient ( $P_{o/w}$ )
	Aqueous Phase	n- Octanol	
Rifabutin	2.76	7.24	2.7

## FORMULATION OF GELATIN NANOPARTICLES:

Nanoparticles were prepared using double desolvation method.

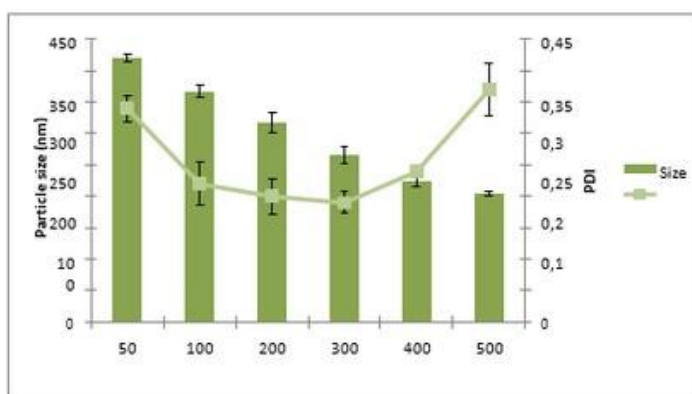
0.2 gm (2.0%) of gelatin was dissolved in 10 ml water by maintaining temperature at  $40 \pm 1^\circ\text{C}$ . Then 10 ml acetone was added in 10 ml gelatin solution as a desolvating agent to precipitate the high molecular mass (HMM) gelatin. Then supernatant was discarded and the HMM was redissolved in 10 ml distilled water under constant stirring at 1200 rpm. Then the pH of the solution was adjusted to the pH 3.0 with the help of HCl. Then we added the drug solution, which was 0.1% w/w. The gelatin was re-desorbed by the drop-by-drop addition of acetone while being stirred at 1200 rpm for 30 minutes using a magnetic stirrer [44].

The formed gelatin nanoparticles were cross linked with 200  $\mu\text{l}$  aqueous glutaraldehyde solution (25%, v/v) at room temp and the solution was stirred for 12 hrs at 1200 rpm. For 2.0 minutes, we sonicated the glutaraldehyde-free nanoparticles after first neutralising the excess with cysteine. After centrifugation at 10,000 rpm for 20 minutes, the particles were cleaned, and the resultant nanoparticles were kept cold

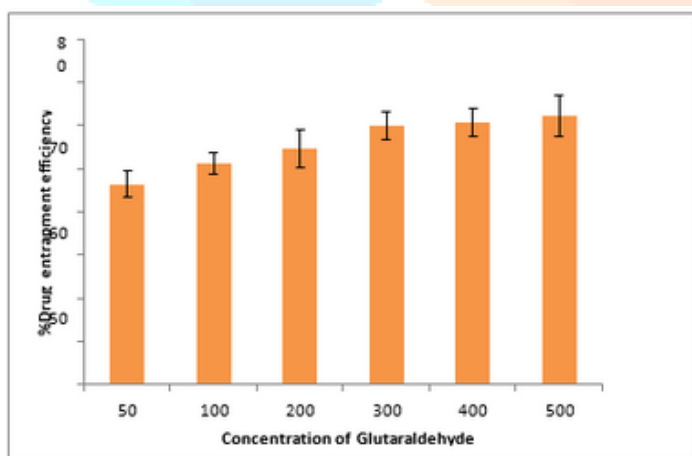
## Optimization of Concentration of glutaraldehyde

Optimization of Concentration of glutaraldehyde for the preparation of gelatin nanoparticles (Type-A 300)

Formulation code	Concentration of Glutaraldehyde	Average size (nm)	% Entrapment efficiency	Polydispersity index
GNP 1	50 $\mu$ l	421 $\pm$ 6.02	46.4 $\pm$ 3.1	0.34 $\pm$ 0.021
GNP 2	100 $\mu$ l	367 $\pm$ 10.1	51.2 $\pm$ 2.4	0.22 $\pm$ 0.034
GNP 3	200 $\mu$ l	318 $\pm$ 16.2	54.7 $\pm$ 4.3	0.20 $\pm$ 0.028
GNP 4	300 $\mu$ l	266 $\pm$ 13.8	59.9 $\pm$ 3.27	0.19 $\pm$ 0.017
GNP 5	400 $\mu$ l	223 $\pm$ 7.6	60.8 $\pm$ 3.2	0.24 $\pm$ 0.005
GNP 6	500 $\mu$ l	204 $\pm$ 3.1	62.4 $\pm$ 4.8	0.37 $\pm$ 0.041



Effect of amount of glutaraldehyde on particle size and PDI for RIF loaded GPA 300



Effect of amount of glutaraldehyde on % EE for RIF loaded GNPA300

## Optimization of Concentration of Gelatin

The concentration of gelatin used to prepare GNPA300 formulations was optimized on the basis of size, PDI and % EE of GNPs. The concentration of gelatin was varied from 1% to 8% w/v. The results showed that 2% w/v gelatin concentration was found to be adequate. At this concentration nanosized GNPs with good size, PDI and entrapment efficiency was obtained. On the contrary, at higher gelatin concentration (3% w/v) though spherical shaped GPs were formed but great variation in size was recorded

Formulation code	Concentration of Gelatin	Average size(nm)	% Entrapment efficiency	Polydispersity index
GNP 1	1%	192±3.5	43.2±2.4	0.14±0.013
GNP 2	2%	267±12.72	58.2±4.1	0.22±0.015
GNP 3	4%	312±12.1	60.9±6.2	0.58±0.031
GNP 4	8%	532±21.7	63.2±3.1	0.65±0.045

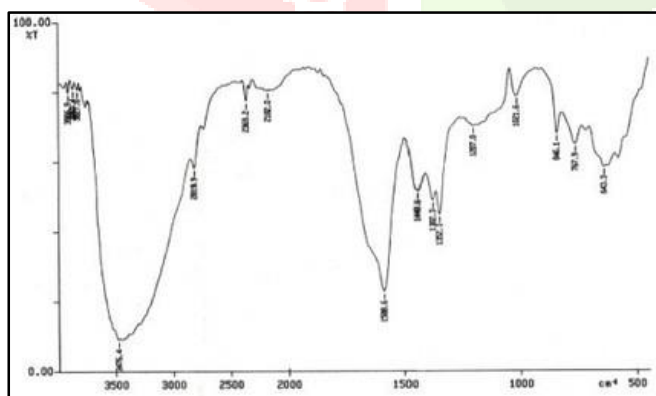
Optimization of Concentration of Gelatin for preparation of gelatin nanoparticles (Type-A 300)

### Mannosylation of Nanoparticles

The method involved ring opening of mannose followed by reaction of its aldehyde group with free amino groups present over the surface of prepared GPs at suitable conditions. This leads to formation of Schiff's base, and mannose became bonded over the nanoparticle surface. Using FTIR analysis, the mannosylated nanoparticles were characterised. Weak N-H stretching at 3460–3580 cm<sup>-1</sup> and significant N-H bending at 1660 cm<sup>-1</sup> in non-mannosylated GPs indicated the existence of primary amine groups. In the instance of MN-GNPs, the N-H bending of secondary amines at 1575 cm<sup>-1</sup> and the C=N stretch at 1505–1465 cm<sup>-1</sup> demonstrated the development of Schiff's base (RCH=N-R bond), showing the establishment of a connection between the mannose ligand and the amine terminal of the nanoparticles. In addition, a wide, intense, and powerful O-H stretch of mannose at 3710–3580 cm<sup>-1</sup> and a significant C-O stretch at 1075 cm<sup>-1</sup> demonstrated the existence of many hydroxyl groups (of mannose) in MN-GNPs. The various peaks of functional groups in FTIR spectra of mannosylated gelatin nanoparticles are tabulated in Table below

Wave number (cm <sup>-1</sup> )	Functional group	Interpretation
3610	O-H stretch	O-H stretch of mannose
1465	C=N stretch	Amide group
1575	N-H bending	Secondary amine
2841.9	C-H bending (in plane)	Methyl and methylene group
1382.3	C-H bending (out plane)	

FTIR spectral illustration of MN-GNPs



FTIR spectrum of mannosylated Gelatin nanoparticles (MN-GNPs)

### Particle size and PDI

The size and PDI of various formulations prepared by gelatin A300 was observed to be 264±11.2 nm (0.241±0.011). The average particle Size of mannosylated GPs (373 ± 23 nm) was quite higher as compared to plain nanoparticles. This could be due to the anchoring of the bulky mannose molecules at the surface of the nanoparticles.

### Surface charge (zeta potential)

The associated zeta potential of these GNPs might be used to infer their surface charge. The positive charge on the surface of gelatin can be explained to the preponderance of the  $\text{NH}_3^+$  group. The high zeta potential of GNPA300 may be related to its large molecular weight and, consequently, its high amine group density at the surface. The medication loading greatly boosted the GNP's net positive. Furthermore, zeta potential is an essential indicator for the stability of GPs suspensions. A high absolute value of zeta potential for Type A gelatin suggests a significant electric charge on the surface of the drug-loaded GPs, which can cause strong repellent forces among particles to prevent aggregation of the GNPs in buffer solution. The decrease in value of zeta potential of GPs on coupling with mannose may be due to a shielding effect of ions, over the charge present at the surface of the nanoparticles.

### Percent drug loading (w/w %)

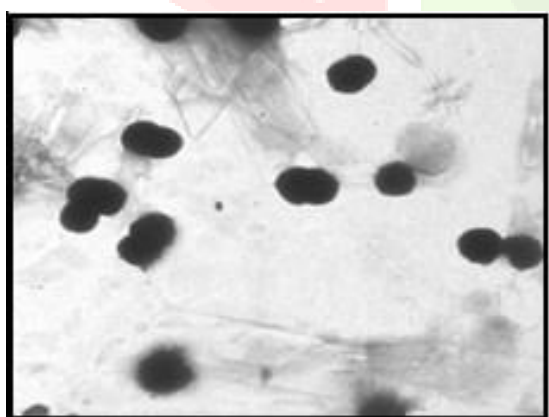
The mannosylation of the nanoparticles has pronounced effect on the encapsulation efficiency. The mannosylation reaction involves the incubation of the nanoparticles with the sodium acetate buffer for 48 h which might leads to the leaching of the drug to the medium and hence responsible for the lower drug entrapment as compared to the plain nanoparticles

### Characterization of RIF loaded Plain and Mannosylated GNPs

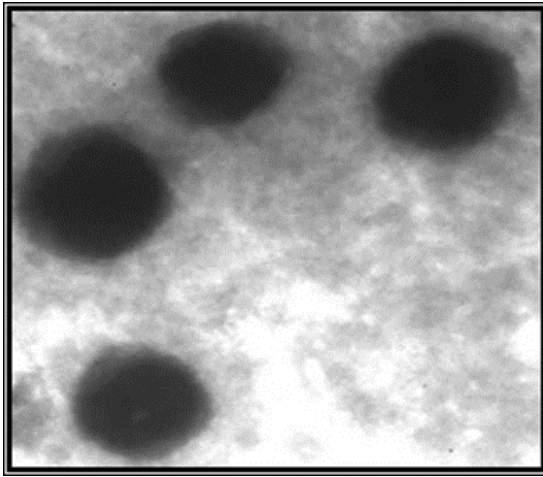
Formulations	Size(nm)	PDI	Drug loading (% w/w)	Actual drug loading (% w/w)	Zeta potential (mV)	
GNP <sub>A300</sub>	RIF	264±11.2	0.241±0.011	59.5±2.82	2.3±0.14	15.32±0.19
	loaded		011			
MN-GNP <sub>s</sub>	RIF	417□31.4	0.232□0.01	52.4±1.68	-	11.46±0.26
	loaded		01			

### TEM study

TEM was used to investigate the size and shape of nanoparticles. TEM photographs suggest that all nanoparticulate preparation were spherical in shape and in nanometric range. However, mannosylated GPs surface was relatively less spherical and smooth in comparison to GNPs



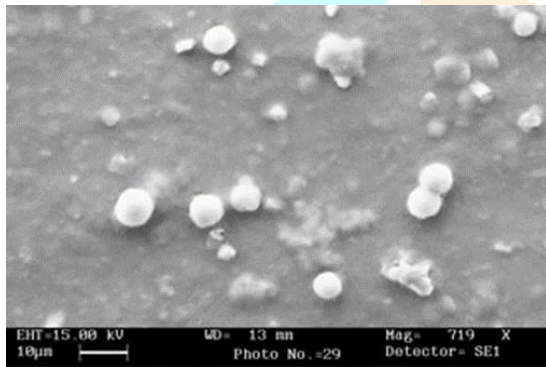
TEM of rifabutin loaded GNPs



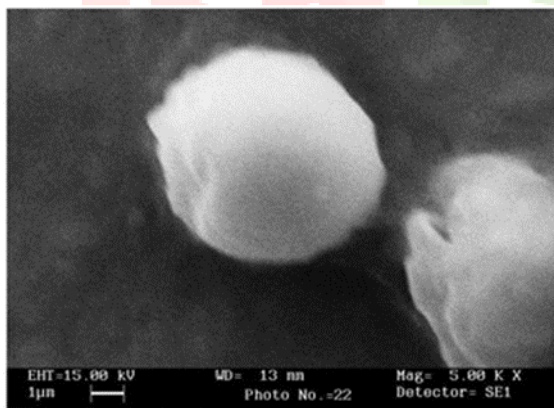
TEM of rifabutin-loaded mannosylated GNPs.

### SEM study

The morphology of gelatin nanoparticles was determined by scanning electron microscopy (SEM). SEM analysis used to characterize the surface and morphological features of nanoparticles. It was found that the surface of GNPs was smooth and spherical

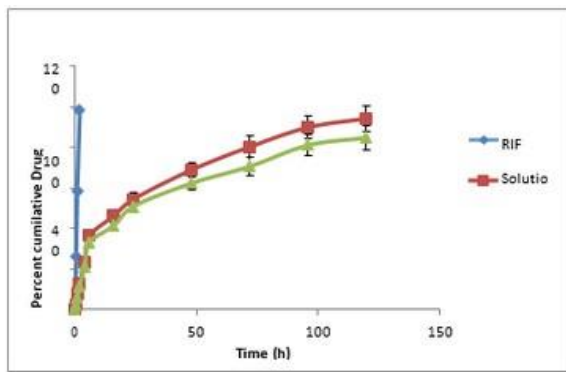


SEM of rifabutin loaded GNPs



SEM of rifabutin-loaded mannosylated GNPs

## In vitro RIF release



In-vitro drug release of various RIF loaded formulations in PBS pH-7.4

## STABILITY STUDIES

The effects of storage time of 3 months at  $5\pm 3^{\circ}\text{C}$  (cold conditions) and  $25\pm 2^{\circ}\text{C}$ ,  $60\pm 5\%$  RH on residual drug content of nanoparticles were determined as per the ICH guidelines.

Formulation code	Initial Drug Content	$5\pm 3^{\circ}\text{C}$			$25\pm 2^{\circ}\text{C}$ , $60\pm 5\%$ RH		
		Drug Content			Drug Content		
		30 days	60 days	90 days	30 days	60 days	90 days
Gelatin nanoparticles (GNPs)	100	99.5 $\pm$ 3.8	98.4 $\pm$ 3.2	97.8 $\pm$ 1.8	98.7 $\pm$ 1.4	98.1 $\pm$ 1.3	97.2 $\pm$ 2.2
Mannosylated Gelatin nanoparticles (MN-GNPs)	100	99.1 $\pm$ 4.2	97.8 $\pm$ 2.5	96.9 $\pm$ 2.1	98.5 $\pm$ 1.6	97.9 $\pm$ 1.6	96.8 $\pm$ 2.3

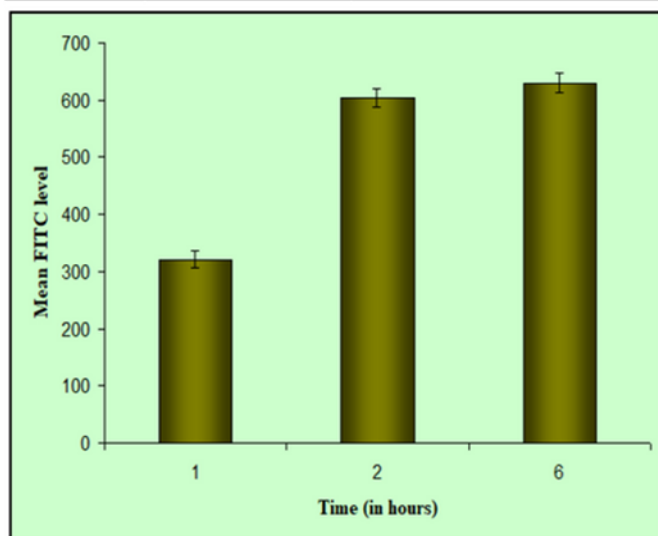
Effects of temperature on % residual drug content of Nanoparticulate formulations

## EX-VIVO STUDIES

Cellular uptake of fluorescein isothiocyanate (FITC) loaded GNPs Results shows that as the time increases, FITC level increases in macrophage cell lines (J774) which may be due to cellular uptake of FITC loaded mannosylated GNPs. This result shows that with rifabutin loaded mannosylated GNPs, high drug concentration can be achieved in alveolar macrophages as it can bypass the metabolism by kupffer cells of liver

Cellular uptake of FITC loaded mannosylated GNPs.

S. No.	Time (hrs)	Mean FITC level
1.	1	321
2.	2	604
3.	6	630



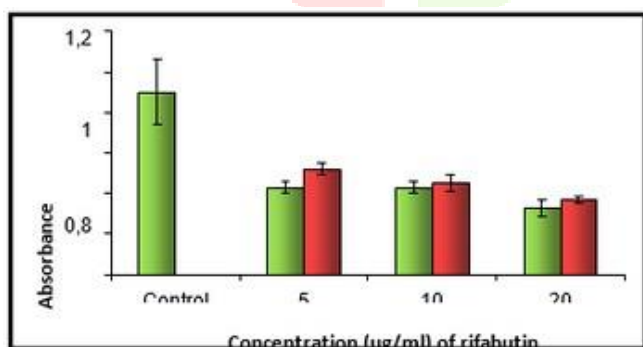
Cellular uptake of FITC loaded mannosylated GNPs

#### MTT cytotoxicity assay:

The mannosylated GNPs at a drug concentration of 1mg/ml showed negligible cytotoxicity in J774 cells possibly due to shielding of the internal cationic charges by surface hydroxyl groups of mannose. The observed cytotoxicity of rifabutin-loaded mannosylated GNPs was much lower than that of rifabutin-loaded solid lipid nanoparticles at all concentrations.

MTT cytotoxicity assay of rifabutin loaded GNPs and MN GNPs

Concentration (ug/ml)	Absorbance	
	Rifabutin loaded mannosylated GNPs	Rifabutin loaded GNPs
5	0.428	0.521
10	0.429	0.450
20	0.326	0.369



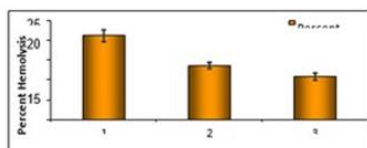
MTT cytotoxicity assay of rifabutin loaded mannosylated GNPs

**Hemolytic Toxicity:** The hemolytic toxicity of rifabutin and rifabutin loaded GNPs was evaluated and the percentage hemolysis on addition of GNPs formulations is shown in fig.16 with the data given in table 13. Rifabutin loaded mannosylated GNPs showed the lowest hemolytic toxicity as compared to rifabutin loaded GNPs, which might be due to the increased hydrophilicity of rifabutin loaded mannosylated GNPs.

Table 13- Percent hemolysis by different formulations on addition to human RBC.

Formulations	Percent Hemolysis after 1hr
Plain rifabutin solution	21.09±1.5
Rifabutin loaded GNPs	13.62±0.8
Rifabutin loaded mannosylated GNPs	10.81±0.9

S.D. ± Mean (n=3)



Percent hemolysis by 1) plain drug 2) GNPs and 3) MN GNPs formulations.

## DISCUSSION

TB is a bacterial infection that is extremely contagious and kills people all over the world. The problems with the present dosage forms of antitubercular medicines may be resolved by designing a site-specific delivery system for antitubercular drugs using surface-modified gelatin nanoparticles. The creation of rifabutin-containing gelatin nanoparticles for the treatment of tuberculosis was the aim of the current effort. Rifabutin-based nano-based medication delivery methods have not been extensively reported. In order to distribute rifabutin to alveolar tissues specifically, Nimje and colleagues successfully created nanoparticles. The synthesis and effective mannosylation of rifabutin-loaded solid lipid nanoparticles (SLNs) were accomplished. Studies of SLNs formulations' ex vivo cellular absorption in alveolar macrophages showed that the mannose coating significantly increased uptake by nearly six times. As an alternative, stearic acid-based SLNs have been investigated as an efficient drug delivery method for anti-tubercular medications and proven to be a solid foundation for lowering dose frequency and enhancing patient compliance. In these present study gelatin nanoparticles were developed because Gelatin is a naturally occurring, flexible biopolymer that has a number of key applications since it is inexpensive, easily accessible, biodegradable, and biocompatible as well as having a large number of active groups.

Initially the preformulation studies of rifabutin was conducted, the focus of preformulation investigations is on the physicochemical concepts that are essential for every new pharmacological molecule and/or proteins/peptides. Their creation of their particular dosage form is also impacted by these characteristics, in addition to the therapeutic effectiveness. The results demonstrated the sample's authenticity and purity. The maximum absorbance of the drug was found to be 275 nm using a UV spectrophotometer, which is in accordance with pharmacopoeia standards. Examining the medication's solubility in various solvents revealed that it was moderately soluble in water, sparingly soluble in ethanol, and soluble in chloroform and methanol. A capillary tube melting point apparatus was used to ascertain the drug's melting point. The melting point was found to be at about 1530 degrees Celsius, which agreed with the pharmacopoeia's listed melting point. Rifabutin was used to create a rifabutin standard curve in PBS with a pH of 7.4 using an ultraviolet spectrophotometer. The Lambert beer law was demonstrated to be followed by rifabutin in the concentration range of 2 to 20 g/ml.

According to the Beer-Lambert law, there will be a linear relationship between an absorbing species' molar concentration and absorbance. It has to do with how light is absorbed and how the qualities of the medium through which the light is travelling. The drug-excipient interaction was found using infrared spectroscopy. The pharmaceutical sample's and excipient's combined IR was found to be within the recommended range. The drug sample can therefore be utilized in the formulation because there is no interaction between it and the excipients anticipated to be employed. Preparation of GNPs was carried out employing two-step desolvation method. Since the nanoparticles produced by this method have been shown to be spherical, have

a small particle size, a low particle density index (PDI), and a good entrapment efficiency, it was decided to use this method for the preparation of GNPs.

Alveolar macrophages serve as the main host for MTb, allowing the pathogen to develop, reproduce, and disseminate throughout the body. As a result, selectively targeting alveolar macrophages proved a successful tactic for curing the illness. But this is possible by surface functionalizing nanocarriers with different ligands that have a particular affinity for the alveolar macrophages. Mannose, a carbohydrate ligand, possesses unique mannose receptors (MR) on macrophages, which aid in the internalisation and targeted delivery of nanocarriers. In the present study Coupling of mannose to GNPs was done. The average particle size of mannosylated GPs was  $373 \pm 23$  nm. The result of zeta potential has been recorded at  $11.46 \pm 0.26$  mV. the electrical double layer that surrounds a nanoparticle in solution and has an electrostatic potential. The zeta potential is what is used to describe this. When the zeta potential of a nanoparticle is between -10 and +10 mV, it is said to be roughly neutral, however when it is larger than +30 mV or lower than -30 mV, it is said to be strongly cationic or anionic. Zeta potential can influence a nanoparticle's propensity to permeate membranes because the majority of biological membranes have a negative charge, with cationic particles typically exhibiting increased toxicity due to rupture of the cell wall. Percent drug loading was found to be  $52.4 \pm 1.68$  which was lesser than RIF loaded GNPs. The amount of drug loaded per unit weight of the nanoparticle is known as loading capacity, and it shows what proportion of the mass of the nanoparticle is made up of drug- encapsulated substance. By dividing the entire weight of the nanoparticles by the total amount of drug contained, one can get the loading capacity (LC %). Drug loading in NP varies greatly and frequently depends on the production technique. In the present study in vitro drug release profiles of RIF loaded GNPs and MN-GNPs were studied using dialysis membrane. Although there is no regulatory or compendial standard, the in vitro release study is a crucial test to evaluate the safety, effectiveness, and quality of nanoparticle-based drug delivery systems. It is challenging to directly compare different systems due to the range of testing methodologies. In our study the release behavior of RIF from the gelatin matrix showed a biphasic pattern that is characterized by an initial burst, followed by a slower sustained release. The GNP formulation showed  $94.2 \pm 6.38\%$  drug release in 120 hours, whereas the MN-GNPs showed  $84.64 \pm 5.76\%$  RIF release at the end of 120 hours. These findings were also similar to the study conducted by Saraogi G et al. The physical stability of gelatin nanoparticle compositions was examined for one month. Nanoparticle stability in terms of shape is defined as the conservation of the original local structure and radius of curvature at the atomic and nanoscales as these dimensions directly impact surface free energy. The retention of nanostructures' catalytic, plasmonic, and mechanical properties is facilitated by this crucial stability descriptor. Because morphological changes affect surface facet percentages, instability occurs in this situation when surface energy declines as a result of shape changes. In the present study all gelatin nanoparticle formulations were tested for their ability to encapsulate at various temperatures, and the results showed that formulations stored under refrigeration (4–80 Degree Celsius) were significantly more stable than formulations stored at room temperature. The physicochemical properties of nanoparticles, such as size, shape, and surface chemistry, as well as the used experimental settings, have an impact on the uptake of the nanoparticles by the cellular systems through a process known as endocytosis. The xanthene dyes category includes the fluorescent dye fluorescein-5-isothiocyanate (FITC). FITC is used to label a variety of biomolecules, including oligo- and polysaccharides, immunoglobulins, lectins and other proteins, peptides, nucleic acids, and nucleotides. Fluorescein-labeled annexin thus can be used to detect and quantitate the apoptotic/dead cells under microscopes or with flow cytometry. The results of research on cellular uptake indicated that FITC levels in macrophage cell lines (J774) increase with time, which may be a result of the body absorbing FITC-loaded mannosylated GNPs. Rifabutin- loaded mannosylated GNPs were found to have significantly reduced cytotoxicity in the MTT experiment than rifabutin-loaded solid lipid nanoparticles at all doses. Rifabutin's hemolytic activity was considerably reduced when it was loaded with GNPs. Rifabutin-loaded mannosylated GNPs displayed the least hemolytic toxicity as compared to rifabutin-loaded GNPs. Therefore, MN-GNPs may be a workable and effective choice for the controlled and secure administration of RIF in tuberculosis-targeted therapy.

The MTT assay method measures the activation metabolism in a cell's mitochondrion and quantifies the impact of nanoparticles on the proliferation of the cell as a way to assess the risk of nanoparticles. In conclusion, the three-week direct colorimetric MTT assay offers a straightforward, quick, and affordable diagnostic and susceptibility test method for *M. tuberculosis*. The growth of bacteria in the media can be seen visually or through spectrophotometric analysis. (41) In the present study mannosylated GNPs at a drug concentration of 1mg/ml showed negligible cytotoxicity in J774 cells.

This result was also in accordance with the study conducted by Upadhyay et al. they reported that Rifabutin loaded alginate sealed GP are not cytotoxic upon uptake by macrophages, they performed MTT viability assay against J774A. The RB loaded GP did not show cytotoxicity to J774 cells, upon 24 h exposure up to a concentration of 80 µg/ml.

Most NPs have hemolytic activity; however it depends on concentration, structure, size, and shape. For instance, the amount of reactive silanol groups exposed on the surface of silica NP is directly related to the size and geometry of the NP. (43) In present study Rifabutin loaded mannosylated GNPs showed the lowest hemolytic toxicity as compared to rifabutin loaded GNPs. The hemolytic activity of plain rifabutin was reduced to a considerable extent when loaded in GNPs. But results for decline in hemolytic activity of rifabutin were obtained when it was present in mannosylated GNPs. This was supposed to be due to the combined effect of slow release of rifabutin and increased hydrophilicity of mannosylated GNPs.

## CONCLUSION

In light of the aforementioned findings, we can draw the conclusion that the proposed drug delivery method containing rifabutin gelatin nanoparticles may show to be a promising route towards the creation of an efficient TB therapy. Additionally, the capacity of this carrier to carry the medication precisely to the site of action may make it easier for the drug's inherent targeting of the infected alveolar cells. Although the exploration of GNPs containing rifabutin increased targeting is a commendable effort, more research is still required to create this carrier for futuristic drug delivery. Additionally, it is envisioned that by searching for newer bioactives, this strategy's potential field of application can be expanded.

## REFERENCES-

1. Dua K, Rapalli VK, Shukla SD, Singhvi G et al. Multi-drug resistant Mycobacterium tuberculosis & oxidative stress complexity: Emerging need for novel drug delivery approaches. *Biomedicine & Pharmacotherapy*; 2018; 107, 1218-1229
2. Global tuberculosis report 2021. Geneva: World Health Organization; 2021. Licence: CC BY-NC-SA 3.0 IGO
3. World Health Organization (WHO), Guidelines for Treatment of Drug-Susceptible Tuberculosis and Patient Care: Essential First-Line Antituberculosis Drugs, WHO, Geneva, Switzerland 2018.
4. Raviglione MC, Harries AD, Msiska R, et al. Tuberculosis and HIV: current status in Africa. *AIDS* 1997; 11(Suppl B):S115–23
5. Adams, Kristin N., John D. Szumowski, and Lalita Ramakrishnan. "Verapamil, and its metabolite norverapamil, inhibit macrophage- induced, bacterial efflux pump-mediated tolerance to multiple anti-tubercular drugs." *The Journal of infectious diseases* 210.3 (2014): 456- 466.
6. Conradie F, Diacon AH, Ngubane N, Howell P, Everitt D, Crook AM, et al. Bedaquiline, pretomanid and linezolid for treatment of extensively drug resistant, intolerant or nonresponsive multidrug resistant pulmonary tuberculosis. *N Engl J Med*. 2020;382(10):893–902.
7. Patil K, Bagade S, Bonde S, Sharma S, Saraogi G. Recent therapeutic approaches for the management of tuberculosis: Challenges and opportunities. *Biomed Pharmacother*. 2018; 99: 735– 45.

8. Jahagirdar PS, Gupta PK, Kulkarni SP, Devarajan PV. Intramacrophage delivery of dual drug loaded nanoparticles for effective clearance of Mycobacterium tuberculosis. *J Pharm Sci* . 2020; 109(7): 2262–70.
9. Makled S, Boraie N, Nafee N. Nanoparticle-mediated macrophage targeting-a new inhalation therapy tackling tuberculosis. *Drug Deliv Transl Res* . 2021; 11(3): 1037–55.
10. Pandit S, Roy S, Pillai J, Banerjee S. Formulation and intracellular trafficking of lipid-drug conjugate nanoparticles containing a hydrophilic antitubercular drug for improved intracellular delivery to human macrophages. *ACS Omega*. 2020; 5(9): 4433–48.
11. Alzahabi KH, Usmani O, Georgiou TK, Ryan MP, Robertson BD, Tetley TD, Porter AE. Approaches to treating tuberculosis by encapsulating metal ions and anti-mycobacterial drugs utilizing nano- and microparticle technologies. *Emerg Top Life Sci*. 2020 ;4(6):581- 600.
12. Costa-Gouveia J, Aínsa JA, Brodin P, Lucía A. How can nanoparticles contribute to antituberculosis therapy? *Drug Discov Today*. 2017 ;22(3):600-607.
13. Ladaviere C, Gref R. Toward an optimized treatment of intracellular bacterial infections: input of nanoparticulate drug delivery systems. *Nanomedicine (Lond)*. 2015;10(19):3033–55.
14. Rao JP, Geckeler KE. Polymer nanoparticles: preparation techniques and size-control parameters. *Prog Polym Sci*. 2011;36(7):887–913.
15. Bamrungsap S, Zhao Z, Chen T, et al. Nanotechnology in therapeutics: a focus on nanoparticles as a drug delivery system. *Nanomedicine*. 2012;7(8):1253–1271
16. Mishra B, Patel BB, Tiwari S. Colloidal nanocarriers: a review on formulation technology, types and applications toward targeted drug delivery. *Nanomedicine*. 2010;6(1):9–24
17. Chopra, H.; Mohanta, Y.K.; Rauta, P.R.; Ahmed, R.; Mahanta, S.; Mishra, P.K.; Panda, P.; Rabaan, A.A.; Alshehri, A.A.; Othman, B.; et al. An Insight into Advances in Developing Nanotechnology Based Therapeutics, Drug Delivery, Diagnostics and Vaccines: Multidimensional Applications in Tuberculosis Disease Management. *Pharmaceuticals* 2023, 16, 581.
18. Grotz, E.; Tateosian, N.; Amiano, N.; Cagel, M.; Bernabeu, E.; Chiappetta, D.A.; Moretton, M.A. Nanotechnology in Tuberculosis: State of the Art and the Challenges Ahead. *Pharm. Res*. 2018, 35, 213.
19. Azimi B, Nourpanah P, Rabiee M, Arbab S. Producing gelatin nanoparticles as delivery system for bovine serum albumin. *Iran Biomed J*. 2014;18(1):34-40.
20. Martin's Physical Pharmacy and Pharmaceutical Sciences : Physical Chemical and Biopharmaceutical Principles in the Pharmaceutical Sciences. Baltimore, MD :Lippincott Williams & Wilkins, 2011.